REPORT

Environmental isotopes as indicators of groundwater recharge, residence times and salinity in a coastal urban redevelopment precinct in Australia

Emily Hepburn[1] · Dioni I. Cendón[2] · Dawit Bekele[3,4] · Matthew Currell[1]

Abstract

Fishermans Bend is an urban redevelopment precinct situated on the Yarra River estuary in Melbourne, Australia. Understanding the hydrogeological system is important for characterising the impacts from legacy contamination and for monitoring the effects of urbanisation on groundwater flow systems and quality. Stable isotopes of water ($\delta^{18}O$, δ^2H) and carbon ($\delta^{13}C$), radioisotopes (^3H, ^{14}C) and other geochemical indicators were used to assess sources of water and salinity in the shallow groundwater. Groundwater in the upper aquifer was predominantly Ca-HCO_3^- dominant, with fresh to brackish salinity—189–3,680 mg/L total dissolved solids (TDS). Localised areas of Ca-SO_4^{2-} and Na-HCO_3^- dominant groundwater were impacted by industrial activities and legacy landfills, respectively. Stable isotopes (e.g. $\delta^{18}O$ −5.7 to −2.9‰) and tritium activities (1.75–2.45 TU) within the aquifer indicate meteoric water recharged by modern rainfall with short residence times. Carbonate dissolution from shell material, and decay of organic waste and methanogenesis in landfill-leachate-impacted bores were shown to enrich $\delta^{13}C$ values up to −4.2‰. In contrast, groundwater in the adjacent/lower aquitard was Na-Cl dominant and saline (19,600–23,900 mg/L TDS), with molar ratios reflective of ocean water, indicating relict emplaced salts. This is consistent with ^{14}C dating of shell material, indicating deposition in a Holocene marine environment. The presence of tritium above background levels (0.20–0.35 TU) in the groundwater, however, suggests a component of modern recharge. Salinity fluctuations within the aquitard at times of peak river level suggest the modern water source is ingress from the adjacent Yarra River.

Keywords Coastal aquifers · Urban groundwater · Stable isotopes · Radioactive isotopes · Australia

✉ Emily Hepburn
   emily.hepburn@rmit.edu.au

1   School of Engineering, RMIT University, GPO Box 2476, Melbourne, VIC 3001, Australia

2   Australian Nuclear Science and Technology Organisation, Locked Bag 2001, Kirrawee, NSW 2232, Australia

3   Global Centre for Environmental Remediation, University of Newcastle, Callaghan, Australia

4   Cooperative Research Centre for Contamination Assessment and Remediation of the Environment (CRC CARE), Melbourne, Australia

Introduction

There is increasing pressure on governments worldwide to utilise vacant, derelict, or former industrial areas proximal to city centres, to solve housing and sustainability challenges (Kotval 2016; UN 2018; USEPA 2018). It is therefore of increasing importance that hydrogeological systems in such areas are well understood, in order to effectively characterise the impacts of legacy contamination, manage water resources, and monitor the effects of urbanisation on groundwater flow systems and quality (Currell et al. 2015; Lee et al. 2016; Han et al. 2017). Such areas are often located on coastlines and/or estuaries, where surface-water bodies and former swamps and wetlands can influence hydrogeological systems and seasonal dynamics (e.g. Bruce et al. 2014; Yeh et al. 2014). In addition, complex characteristics often associated with former industrial areas can make understanding the hydrogeological system a

challenging task; for example, remnant underground infrastructure may artificially recharge and/or drain urban groundwater, heterogeneous artificial fill may overlie the natural sediments and modify groundwater flow paths, and multiple contamination sources, such as legacy landfills and industrial activities, may impact groundwater salinity and geochemistry (e.g. Christensen et al. 2001; Cossu 2013; Schirmer et al. 2013; Han et al. 2016).

Documenting solute origins, groundwater flow paths, recharge and residence times is fundamental to understanding complex hydrogeological systems (Cartwright et al. 2007). Stable- and radioisotopes of water, used in combination with other geochemical indicators (e.g. major ion compositions and physico-chemical characteristics of the groundwater), are recognised as valuable tools in this regard. These tracers can help to determine salinity sources and residence times in groundwater systems within urban and other environments (e.g. Hughes et al. 2011; Vázquez-Suñé et al. 2010; Cendón et al. 2015), including estuaries (Price et al. 2012). In this study, geochemical indicators and isotopes were used to better understand hydrogeological conditions and processes at Fishermans Bend, a large urban redevelopment precinct situated on the Yarra River estuary in Melbourne, Australia (DELWP 2017). The region encompasses 240 ha of former industrial land and contains several historical landfills and industries which have contaminated the soils and groundwater to varying degrees (Hepburn et al. 2018). Little is currently known about groundwater age, recharge and residence times in the redevelopment precinct, as there has been no previous hydrochemical/isotopic study of the aquifer system. These are major knowledge gaps which require addressing to accurately constrain site-based groundwater contamination, and develop effective management/remediation strategies during redevelopment of the precinct.

The main objectives of this study were to: (1) determine the major sources of water and salinity in the groundwaters of two distinct hydrofacies (an upper aquifer and an adjacent and underlying aquitard); (2) investigate evidence for modern recharge/leakage to the lower aquitard; and (3) document controls on groundwater recharge, discharge and residence times. Previous hydrogeological investigation hypothesised that solutes within the lower aquifer derive from relict marine water (e.g. Neilson 1992). However, there has subsequently been no sampling of the water for environmental isotopes, which holds the potential to resolve this question, and in general gain a clearer understanding of the timescales and mechanisms of groundwater recharge and solute evolution. The results of this study will provide a better understanding of the hydrogeological system at Fishermans Bend and provide valuable context regarding natural versus contamination-derived salinity in groundwater. Overall the study seeks to provide a guide for hydrochemical investigation techniques that allow baseline characterisation of groundwater recharge

and solute origins within urban redevelopment precincts, and guidance with respect to the use of environmental isotopes in similar settings (e.g. coastal sedimentary aquifers impacted by various contamination sources). At the local level, the study seeks to increase consistency and efficiency in individual site investigations undertaken at Fishermans Bend as redevelopment progresses, by providing better regional context of the hydrogeological system, including the recharge and flow regime and natural/anthropogenic sources of solutes.

Background and setting

Land use history

Fishermans Bend is located approximately 1 km southwest of the Central Business District of Melbourne, Australia (Fig. 1), and is currently undergoing redevelopment from historically industrial to medium/high density residential land (DELWP 2017). The area was developed from shallow coastal swampland into industrial land during the latter half of the nineteenth century, with automotive and aircraft manufacturing, metal plating fabrication, and plastic and packaging manufacturing prominent among the many local industries (Golder Associates 2012). Sand quarrying was common across the area prior to the 1920s, after which landfilling occurred between the 1930s and 1990s with wastes sourced from municipal, industrial, construction and/or demolition activities (Hepburn et al. 2019a, b).

Geology and hydrogeology

Fishermans Bend is located near the mouth of the Yarra River, on Quaternary river-delta sediments (Fig. 1). The shallow subsurface is typically underlain by artificial fill which ranges from being absent to approximately 5 m thick (Neilson 1992). Holdgate and Norvick (2017) characterised the geological evolution of the delta, showing that the uppermost natural units comprise Holocene transitional alluvial/marine sediments. The uppermost unit consists of the Port Melbourne Sand which comprises fine- to medium-grained sands, typically 5–10 m thick with significant shell beds more common towards the base of the unit (Neilson 1992). ^{14}C dating of shell material in the lower and upper beds indicate ages ranging from 8,075 to 2,760 years BP, respectively (Holdgate and Norvick 2017). The Port Melbourne Sand acts as an unconfined high-yielding aquifer, with a shallow water table typically between 1 and 3.5 m below ground surface (Neilson 1992). Groundwater salinity in this unit has been reported as fresh to brackish, varying from 91 to 2,971 mg/L total dissolved solids (TDS; AECOM 2016). The groundwater varies from oxygen-rich to reducing—dissolved oxygen (DO) from 0.01 to 5.72 mg/L, and redox potential (Eh) from −56 to
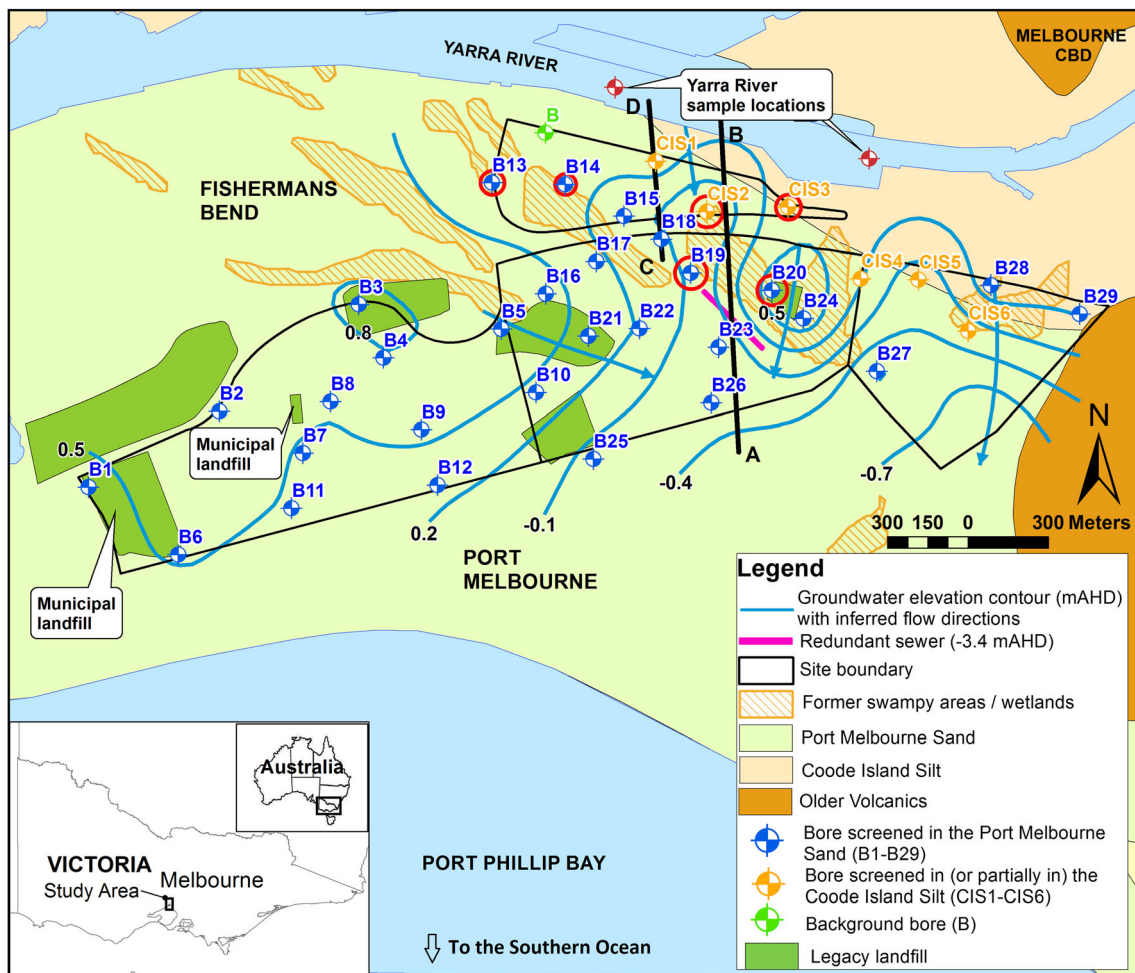
Fig. 1 Map of Fishermans Bend including legacy landfills, swampy areas (City of Melbourne map, 1864, cited in AECOM 2015), redundant sewer (fuchsia-colored line), cross-section A–B and cross-section C-D. Hydrographs (bores circled in red)

>500 mV—and has a typically neutral pH (median = 6.56, range: 2.96–7.56), with localised areas of low pH associated with industrial contamination (AECOM 2016).

The Coode Island Silt sits stratigraphically below the Port Melbourne Sand (although with some contemporaneous deposition) and is comprised of soft, silty clays with variable amounts of marine shells and high organic matter (e.g. plant material; Smith and Milne 1979). Contact between the Port Melbourne Sand and the Coode Island Silt is typically sharp but can be gradational, particularly in the northeast of Fishermans Bend where the units are lateral equivalents, deposited at different water depths (Holdgate and Norvick 2017). Transitional material is often present at the base of the Port Melbourne Sand and typically consists of sandy clay and/or clayey sand. Recent ^{14}C dating of shell material in the upper beds of the Coode Island Silt resulted in ages between 8,254 and 6,555 years BP (Holdgate and Norvick 2017). The unit acts as an aquitard, 20–25 m thick, with high porosity and low permeability (Hancock 1992). Groundwater in this unit has been reported as reducing (median Eh = −24 mV) with

neutral pH (median = 6.72) and high salinity (median = 19,490 mg/L TDS; AECOM 2016). Evidence for methanogenesis occurring in this unit (including presence of dissolved methane in groundwater) was reported in Hepburn et al. (2019b).

Climate and surface water

The climate in Melbourne is semi-arid, with an annual precipitation of 663 mm and a potential evapotranspiration (PET) of approximately 1,010 mm (BOM 2018). Precipitation is relatively consistent throughout the year; mean monthly precipitation varies from 43 mm in January (summer) to 65 mm in November (spring); however, 41% of total PET occurs in summer (December–February, mean temperature = 25 °C) compared to only 13% in winter (June–August, mean temperature = 14 °C; BOM 2018). These seasonal changes in PET are likely to have a major influence on recharge potential to groundwater (e.g. greater in winter when PET is lower). The Yarra River flows from east to west, is situated immediately

north of Fishermans Bend, and is tidally driven by Port Phillip Bay which has a narrow connection to the Southern Ocean in the south (EPA Victoria 2013; Fig. 1). As such, ocean water is present as a saline wedge at the base of the river and typically extends beyond Fishermans Bend upstream to the east (EPA Victoria 2013). A thin layer of relatively freshwater is present at the surface (typically 1–2 m thick) with a mixed zone in between the fresh and saline layers (EPA Victoria 2013). River flow is permanent, but is generally higher in winter and spring, and lower in summer and autumn (Beckett et al. 1982). The Yarra Estuary is narrow and naturally shallow, with a maximum depth of 8 m (Bruce et al. 2011).

Materials and methods

Sample collection, slug tests and laboratory analysis procedures

Groundwater samples were collected from 36 shallow monitoring bores (constructed with 50-mm diameter PVC, with slotted screen intervals), over three sampling campaigns in May 2016, August 2016 and May 2017. Most bores were screened in the Port Melbourne Sand aquifer (sample codes B1–B29) with four bores screened in the Coode Island Silt (CIS1–CIS4) and two bores screened through both the Port Melbourne Sand and the Coode Island Silt—i.e. mixed/ transitional material; sample codes CIS5 and CIS6 (see Figs. 1 and 2). One background bore screened in the Port Melbourne Sand and located upgradient from any known contaminant sources was also sampled (sample code B). Information including bore depths, screened intervals and lithology are presented in Table S1 of the electronic supplementary material (ESM). Hydraulic conductivity values were estimated from slug tests

conducted in five bores within the Port Melbourne Sand (B5, B16, B17, B21 and B22) and two bores within the Coode Island Silt (CIS1 and CIS3) (see Table S2 and Fig. S1 of the ESM, for full method details and results). Samples were collected using a low-flow bladder pump with dedicated low-density poly ethylene (LDPE) tubing. New tubing and bladders were used for each sample. Prior to sample collection, standing water level was measured using a Solinst interface probe and field parameters were monitored in purged water within a flow-cell (in-line). Stabilisation of water levels and parameters was achieved prior to sample collection, in accordance with standard No. 5667–11 (ISO 2009). A total of 49 samples were analysed for TDS, alkalinity and major ions and were collected in 250-ml plastic bottles. In addition, 21 samples were analysed for dissolved methane and were collected in air-tight 40-ml vials. All samples were stored at 4 °C before being submitted to Australian Laboratory Services for analysis via PC Titrator (alkalinity), dual column gas chromatography with flame ionization detector (dissolved methane), and inductively coupled plasma mass spectrometry (cations). Anions were analysed by Discrete Analyser, following APHA 4500 methods (2017). Charge balances were all within 10% (86% of samples within 5%), except for one sample location (B27) where balances were −19.2% in May 2016 potentially due to high organic matter content (Siegel et al. 2006). Groundwater salinity, alkalinity and major ion data are shown in Table 1. Dissolved methane data are shown in Table 2.

A total of 49 samples for water stable isotopes (δ^2H and δ^{18}O) were collected in May 2016 and May 2017, in clean 250-ml plastic bottles and filtered through 0.45-µm in-line filters (Aquapore). Samples were analysed using an established Picarro Cavity Ring-Down Spectroscopy method at the Australian Nuclear Science and Technology

Fig. 2 Cross section A–B showing the major geological units of interest to this study, and the Yarra River. Bore screen intervals are marked using horizontal lines
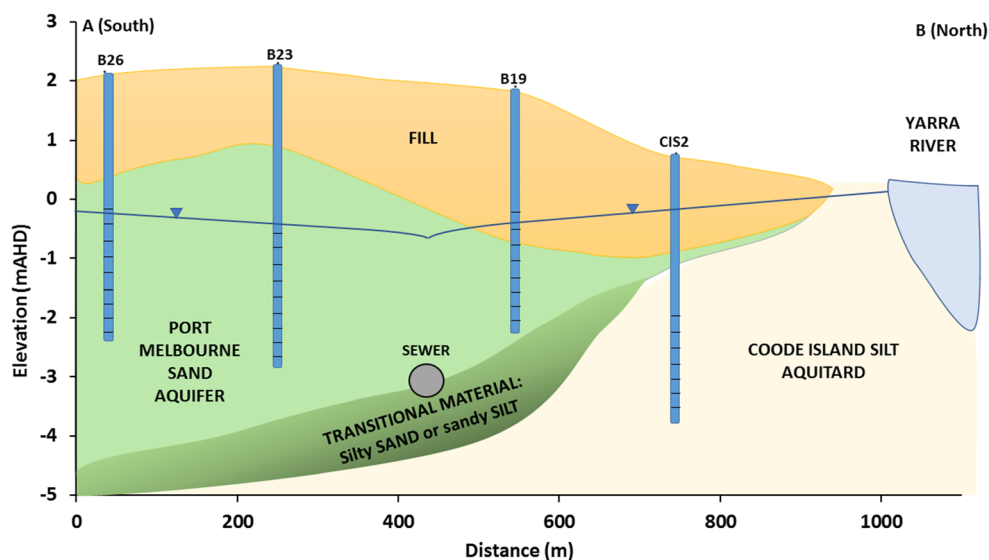
Table 1 Major ion and stable isotope results (major ions are in mmol/L)

Bore	Unit	Sample date	TDS (mg/L)	pH	Na	Mg	K	Ca	Cl	SO_4^{2-}	HCO_3^-	δ^2H (‰)	$\delta^{18}O$ (‰)
B	PMS	May 2016	143	6.64	0.57	0.16	0.10	0.62	0.31	0.06	1.57	−24.2	−4.3
B1	Fill	May 2016	3,680	6.86	36.8	3.41	5.04	0.80	24.1	0.31	26.9	−21.1	−4.4
B2	Fill	May 2016	2,240	6.88	19.2	3.13	1.07	1.75	9.11	0.01	23.9	−23.8	−4.5
B3	Fill	May 2016	1,360	7.11	6.92	4.11	1.10	4.27	3.30	2.02	15.0	−24.6	−4.5
		May 2017	1,560	7.09	7.48	4.24	1.13	4.49	3.95	3.32	15.3	−24.6	−4.5
B4	Fill/PMS	May 2017	900	6.70	2.17	1.93	0.36	5.29	0.68	2.65	8.77	−21.5	−4.0
B5	Fill/PMS	May 2016	1,540	6.50	9.40	4.36	1.41	2.50	4.46	0.01	18.2	−24.3	−4.4
		May 2017	1,470	6.92	9.26	3.95	1.33	2.12	4.82	0.01	18.4	−24.1	−4.4
B6	PMS	May 2016	2,970	6.56	21.8	5.60	1.89	10.7	13.5	10.0	18.2	−26.4	−4.8
B7	PMS	May 2016	1,490	7.00	6.39	2.02	0.79	5.91	4.71	1.26	15.4	-	–
B8	PMS	May 2017	885	6.38	2.17	1.23	0.43	5.21	1.66	3.54	6.69	−25.3	−4.6
B9	PMS	May 2016	1,130	7.13	5.83	1.32	0.61	4.64	2.45	4.08	6.92	−28.8	−5.1
B10	PMS	May 2016	513	6.18	2.04	0.99	0.23	1.85	0.79	1.17	4.26	−26.3	−4.9
		May 2017	342	5.80	1.39	0.66	0.18	1.32	0.59	0.80	2.95	−26.4	−5.0
B11	PMS	May 2016	483	6.38	1.65	0.25	0.23	2.52	0.42	1.23	4.00	−26.2	−4.8
B12	PMS	May 2016	1,100	6.04	4.13	1.19	0.51	5.69	4.01	3.74	5.79	−23.4	−4.2
		May 2017	938	6.23	3.44	0.95	0.46	4.69	3.07	2.82	6.15	−23.0	−4.1
B13	PMS	May 2016	484	7.05	2.17	0.99	0.31	2.35	0.56	1.29	5.41	−26.7	−4.8
B14	PMS	May 2016	449	6.70	2.04	0.70	0.51	1.65	0.73	0.72	4.31	−14.9	−2.9
		May 2017	319	6.26	3.04	0.91	0.51	2.05	0.82	1.25	5.90	−19.7	−3.7
B15	PMS	May 2016	870	6.52	5.79	1.15	0.33	3.02	2.20	2.44	6.13	−24.1	−4.4
B16	Fill/PMS	May 2016	1,650	7.22	9.48	2.72	0.61	7.69	3.50	6.66	11.8	−25.3	−4.5
		May 2017	1,600	7.19	10.2	3.00	0.59	5.24	3.55	5.07	13.6	−26.6	−4.8
B17	PMS	May 2016	779	5.99	4.05	1.03	0.18	3.12	0.96	3.11	4.28	−22.0	−4.0
		May 2017	435	6.30	6.70	0.74	0.20	2.12	1.18	2.73	5.69	−23.6	−4.4
B18	PMS	May 2016	753	5.62	5.13	1.44	0.38	1.82	3.70	3.15	1.92	−23.1	−4.3
B19	PMS	May 2016	1,940	6.26	15.3	2.26	0.69	5.12	17.1	6.52	2.44	−23.8	−4.3
B20	PMS	May 2016	2,280	6.67	20.8	3.04	1.00	3.24	20.3	0.01	13.5	−21.1	−3.7
B21	PMS	May 2016	1,830	7.05	8.35	5.92	0.92	7.31	2.03	10.3	10.1	−24.6	−4.4
		May 2017	1,750	6.35	6.35	5.31	0.87	6.94	1.44	11.0	8.92	−24.6	−4.5
B22	PMS	May 2016	1,040	6.12	1.17	0.86	0.20	8.31	0.37	7.97	1.56	−22.5	−4.3
		May 2017	569	5.75	0.78	0.45	0.10	3.77	0.62	3.53	1.77	−26.0	−4.8
B23	PMS	May 2016	834	5.95	1.96	1.28	0.31	5.51	1.02	5.52	3.90	−25.6	−4.7
		May 2017	189	5.86	0.61	0.12	0.01	0.75	0.34	0.28	1.48	−32.5	−5.7
B24	PMS	May 2016	2,170	7.39	29.3	1.89	0.74	1.87	6.35	4.36	19.0	−25.1	−4.5
		May 2017	1,050	6.71	19.4	3.04	1.13	2.27	6.54	5.67	13.1	−25.8	−4.7
B25	PMS	May 2016	930	6.90	4.00	1.19	0.31	4.39	2.43	2.48	7.36	−26.8	−4.8
B26	PMS	May 2016	1,460	2.96	2.57	1.40	0.23	4.47	0.82	10.3	0.01	−24.6	−4.4
B27	PMS	May 2016	1,480	6.56	7.48	1.93	0.61	2.27	8.15	1.34	5.75	−26.6	−4.7
B28	PMS	May 2016	1,040	6.73	2.74	2.88	0.61	3.47	3.84	0.07	11.8	−24.4	−4.6
B29	PMS	May 2016	2,650	6.51	14.4	8.35	1.05	12.3	4.01	19.7	7.31	−22.2	−4.0
CIS1	CIS	May 2016	22,300	6.86	326	48.1	5.68	9.66	347	3.77	51.3	−18.8	−3.4
CIS2	CIS	May 2016	23,900	6.76	316	40.0	4.86	9.26	330	5.04	48.0	−18.3	−3.1
CIS3	CIS	May 2016	19,600	6.48	258	39.6	4.86	8.43	293	5.52	40.0	−21.7	−3.8
CIS4	PMS/CIS	May 2016	6,210	6.56	48.3	15.8	2.53	19.9	84.3	14.8	6.11	−22.7	−4.0
		May 2017	7,300	6.74	66.1	8.48	1.53	18.6	93.7	14.4	7.93	−22.6	−4.1
CIS5	PMS/CIS	May 2016	8,390	6.67	90.9	12.9	1.30	20.9	126	13.3	9.78	−21.5	−3.9
CIS6	PMS/CIS	May 2016	2,200	6.75	24.0	3.70	1.13	2.17	23.0	1.69	9.18	−22.3	−4.1
Yarra River		July 2018	–	–	–	–	–	–	344	–	–	−3.50	−1.0
Yarra River		July 2018	–	–	–	–	–	–	322	–	–	−9.50	−2.0

PMS Port Melbourne Sand; CIS Coode Island Silt; - not measured

Organisation (ANSTO). Results are reported against Vienna Standard Mean Ocean Water (VSMOW) using delta (δ) notation and are accurate to ±1‰ for δ^2H and ± 0.15‰ for $\delta^{18}O$. All water stable isotope results are presented in Table 1. A total of 26 samples for carbon stable isotopes ($\delta^{13}C_{DIC}$) were collected in May and August 2016 in preconditioned gas sealed 12-ml glass vials (Exetainer) and field filtered through 0.20-µm sterile syringe filters (Minisart) without any

Table 2 Radioisotope, $\delta^{13}C_{DIC}$, Ca/Cl and K/Cl ratios, and dissolved methane results; bores are grouped according to whether: (1) they are impacted by landfill leachate; (2) shell beds are present; and (3) neither

Bore	Unit	Sample date	Tritium (TU)	$\delta^{13}C_{DIC}$ (‰)	^{14}C (pmc)	Ca/Cl	K/Cl	Dissolved CH$_4$ (mg/L)
B1[a]	Fill	May 2016	–	−4.20	–	0.03	0.21	3.9
B2[a]	Fill	May 2016	–	+7.90	–	0.19	0.12	10
B5[a]	Fill/PMS	May 2016	–	−10.9	–	–	–	–
		August 2016	1.88	−10.6	74.35	0.51	0.25	10
B6[a]	PMS	May 2016	–	−16.4	–	–	–	–
		August 2016	1.86	−9.30	82.01	0.87	0.11	0.04
B20[a]	PMS	May 2016	2.02	−9.40	74.41	0.16	0.05	7.6
B24[a]	PMS	May 2016	1.75	−12.7	83.94	0.29	0.12	0.42
B7[a,b]	PMS	May 2016	–	−8.20	–	–	–	–
		August 2016	2.13	−6.00	71.65	1.4	0.14	0.14
B9[a,b]	PMS	May 2016	–	−15.4	–	1.9	0.25	0.06
B16[b]	Fill/PMS	May 2016	–	−19.5	–	2.2	0.18	0.05
B21[b]	PMS	May 2016	–	−19.4	–	3.6	0.45	0.02
B22[b]	PMS	May 2016	–	−16.8	–	23	0.56	<0.01
B23[b]	PMS	May 2016	1.79	−12.5	38.59	5.4	0.30	0.01
B27[b]	PMS	August 2016	2.39	−12.1	31.14	0.28	0.08	–
B29[b]	PMS	May 2016	–	−10.2	–	3.1	0.26	0.03
CIS1[b]	CIS	May 2016	0.20	−4.20	56.54	0.03	0.02	1.2
CIS2[b]	CIS	May 2016	0.25	−12.2[c]	72.79	0.03	0.01	–
CIS3[b]	CIS	May 2016	–	−13.3	–	–	–	–
		August 2016	0.35	−9.60	71.30	0.02	0.01	0.69
CIS6[b]	PMS/CIS	May 2016	–	−11.6	–	–	–	–
		August 2016	2.27	−10.8	35.97	0.09	0.04	0.04
B14	PMS	August 2016	2.45	−14.6	62.11	2.5	0.70	<0.01
B18	PMS	May 2016	–	−13.5	–	0.49	0.10	0.04
B19	PMS	May 2016	1.88	−18.5	61.88	0.30	0.04	0.17
B26	PMS	May 2016	1.94	−17.3	59.48	5.5	0.28	<0.01
B28	PMS	May 2016	–	−11.2	–	0.90	0.16	1.4

[a] Landfill leachate impacted bores

[b] Bores with shell beds present

[c] $\delta^{13}C_{DIC}$ are graphite derived values from the fraction used for the radiocarbon measurement. All other values are determined using EA-IRS

PMS Port Melbourne Sand; CIS Coode Island Silt; - not analysed

additives. $\delta^{13}C_{DIC}$ values were measured with a Delta V Advantage Isotope Ratio Mass Spectrometer at ANSTO, following the method outlined in Assayag (2006). Results are reported relative to V-PDB and are accurate to ±0.3‰.

A total of 14 samples for tritium and radiocarbon analysis were collected in May and August 2016 in clean 2-L plastic bottles, filtered through 0.45-μm in-line filters (Aquapore). Samples for tritium were distilled and electrolytically enriched prior to being analysed by liquid scintillation spectrometry at ANSTO (Iverach et al. 2017). Tritium results are expressed in tritium units (TU), and have 1σ uncertainties between 0.04 and 0.36, with a quantification limit of 0.05 TU. Measurement of radiocarbon activities was done on graphite targets by accelerator mass spectrometry, using the ANSTO

2MV tandem accelerator STAR (Fink et al. 2004), following methods described in Cendón et al. (2014). Percent modern carbon (pMC) results are provided in Table S3 of the ESM, following reporting guidelines in Stuiver and Polach (1977). The reported pMC results were de-normalised and used as (pMC), using the equation provided for measurements based on the $^{14}C/^{12}C$ ratio by Mook and van der Plicht (1999). All radioisotope (and $\delta^{13}C_{DIC}$) results are shown in Table 2.

Mixing calculations

Possible mixing proportions of Yarra River water and fresh meteoric water in groundwater were estimated according to mass balance in a two end-member system, using two

independent indicators (chloride and $\delta^{18}O$) as outlined in Vázquez-Suñé et al. 2010 and Eqs. (1) and (2), respectively:

$$f_{river} = \frac{Cl^-_{sample} - Cl^-_{fresh}}{Cl^-_{river} - Cl^-_{fresh}} \qquad (1)$$

$$f_{river} = \frac{\delta^{18}O_{sample} - \delta^{18}O_{fresh}}{\delta^{18}O_{river} - \delta^{18}O_{fresh}} \qquad (2)$$

where f_{river} represents the fraction (between 0 and 1) of Yarra River water estimated in a groundwater sample of mixed origin, with the remainder assumed to comprise fresh groundwater of meteoric origin. The end-member results for the Yarra River were chosen using average values of chloride and $\delta^{18}O$ from two samples collected in July 2018 from different locations (within the bounds of the study area; see Fig. 1) from depths of approximately 3 m below the surface (i.e. in the mixed zone—see section 'Climate and surface water'). The end-member results for freshwater used the average rainfall chloride for Melbourne of 0.15 mmol/L and the $\delta^{18}O$ value of Melbourne average weighted rainfall of −4.7‰ (Hollins et al. 2018).

Results

Groundwater flow direction, levels and hydraulic conductivities

Groundwater flow predominantly converges in the central part of Fishermans Bend towards a legacy (redundant) sewer which inadvertently acts as a regional groundwater drain (Fig. 1). The sewer is located at a depth of −3.4 m Australian Height Datum (AHD) and is an open cracked ceramic conduit (300 mm

diameter; AECOM 2015). The effect of the sewer is to redirect groundwater away from a topography-driven drainage path towards the Yarra River, and to lower groundwater levels below sea level. No seasonal changes in this flow direction were observed during eight separate monitoring events over an 18-month period between November 2015 and May 2017 (Table S4 of the ESM). Hydraulic gradients across the study area ranged between 0.0012 and 0.0014 (mean = 0.0013), reflecting the flat topography. Using Hvorslev's method (Hvorslev 1951), estimated hydraulic conductivity values in the Port Melbourne Sand varied from 1.7 to 23 m/day, consistent with the range reported in A. Cooney (unpublished report, Geological Survey Victoria 1984, cited in Leonard 2006) of 0.86–43 m/day. In contrast, significantly lower hydraulic conductivity values of 0.0005–0.003 m/day were estimated for the Coode Island Silt, consistent with low permeabilities reported in Hancock (1992).

Hydrographs for three bores screened in the Port Melbourne Sand aquifer (B13, B14 and B20) over a 21-month period are presented in Fig. 3, along with daily rainfall. Groundwater levels in the aquifer positively correlated with rainfall and typically fluctuated between −0.3 and 0.8 mAHD. Groundwater levels were generally higher in winter and early spring. Two significant rain events (i.e. rainfall greater than 40 mm) in December 2017 and January 2018, resulted in sustained higher groundwater levels over the summer. Similar patterns in groundwater level were observed within data collected from multiple manual gauging events over an 18-month period between November 2015 and May 2017 (Table S4 of the ESM). These data also indicated an inverse relationship between groundwater level and salinity in twelve bores screened in the Port Melbourne Sand aquifer (bores B2, B6, B8, B10, B11,
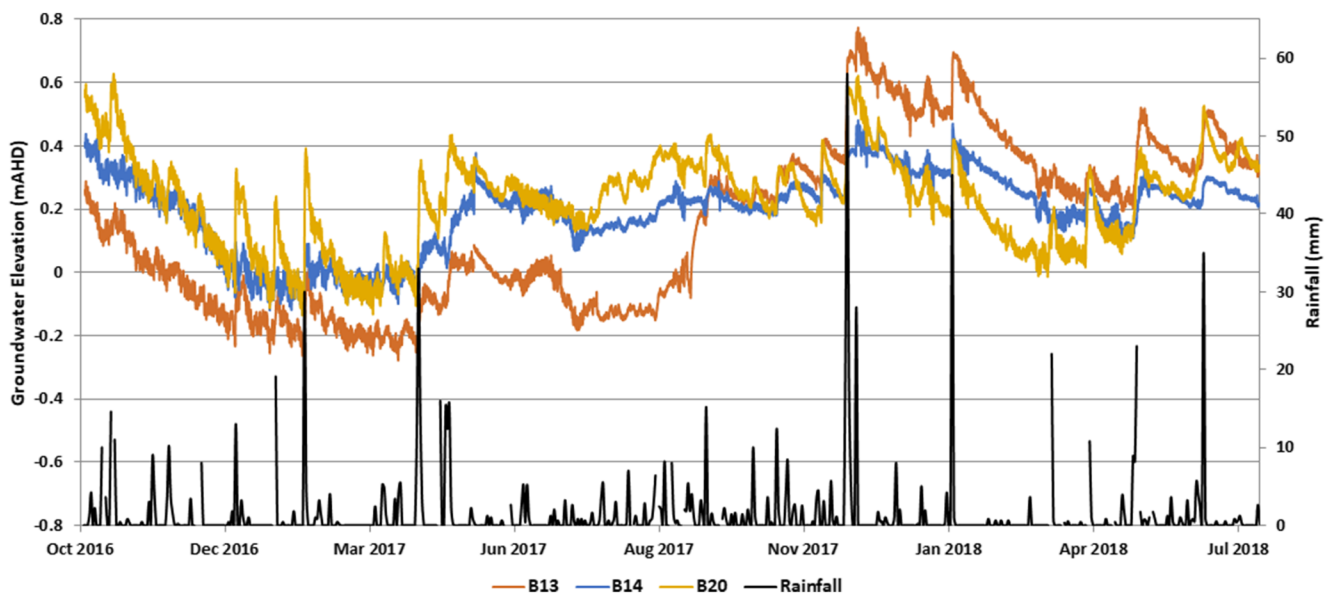

Fig. 3 Hydrographs for three bores (B13, B14, B20) within the Port Melbourne Sand aquifer over a 21-month period, including daily rainfall (source: BOM 2018)

B15, B18, B20, B22, B23, B25, B26; Fig. 1), with R^2 values between 0.31 and 0.94 (mean R^2 value = 0.57).

In addition, groundwater level and salinity were monitored at high frequency (every second) in one bore (B18) screened in the Port Melbourne Sand and located within 500 m of the Yarra River, over a 5-day period, along with river elevation (Fig. 4a,b). Minimal rainfall occurred during the monitoring period (total 3.8 mm) which had no effect on groundwater level; instead groundwater levels positively correlated with river levels (Fig. 4a), demonstrating a degree of tidal influence on groundwater within the Port Melbourne Sand, at least within 500 m from the river. Five separate manual gauging events between April 2016 and May 2017 provide evidence of salinity stratification and mixing within this bore. For example, when groundwater levels were low (approximately −0.3 mAHD), mean TDS in the upper and lower sections of the bore (monitored at the top and base of the bore's screened interval, which was between 2.5 and 4.0 m below ground level) were 263 and 964 mg/L, respectively. In contrast, when groundwater level was higher (approximately 0.0 mAHD), mean TDS in the upper and lower sections were 213 and 262 mg/L, respectively (Table S4 of the ESM). These periodic TDS fluctuations likely indicate that the well is screened within the transition zone between fresh and more saline groundwater, and that tidal loading results in cyclic landward and seaward (i.e., Yarra Estuary) movement of the zone (Fig. 5).

Hydrographs over a 5-month period for two bores located adjacent to the Yarra River and screened across the water table, between 2 and 5.5 m depth below ground level in the Coode Island Silt aquitard (CIS2 and CIS3) are presented in Fig. 6a, along with daily rainfall and river elevation. Groundwater levels in the aquitard fluctuated between −1.0 and −0.4 mAHD in bore CIS2 and between 0.3 and 0.5 mAHD in bore CIS3 and showed some correspondence with rainfall and river elevation—e.g. short-term decreases in TDS corresponding to peaks in river level (Fig. 6). To investigate whether these correlations may be attributable to recharge (e.g. via direct rainfall infiltration or vertical leakage from the Port Melbourne Sand and/or ingress from the river), or whether they are solely the result of pressure changes (e.g. tidal loading), salinity was also measured in bore CIS2 to assess its correlation with water level. Groundwater levels and salinity in bore CIS2 are presented in Fig. 6b, over a 25-day period during which rainfall and river levels peaked. Salinity was generally stable at approximately 27,200 mg/L TDS; however, a slight decrease to 27,100 mg/L TDS is observable during peak rainfall (23 mm/day) when groundwater levels increased from −0.7 to −0.5 mAHD. Similarly, during peak river levels (1.1 mAHD), fluctuations in salinity were observed—e.g. from 27,000 to 27,500 mg/L TDS on 13 July 2016 when groundwater levels increased from −0.65 to −0.50 mAHD. These data indicate minor recharge or ingress of water to the aquitard in conjunction with high rainfall and/or river levels; consistent with the presence of tritium (albeit at low concentrations, see section 'Isotopic data: δ^{18}O, δ^{2}H, δ^{13}C, tritium and radiocarbon').
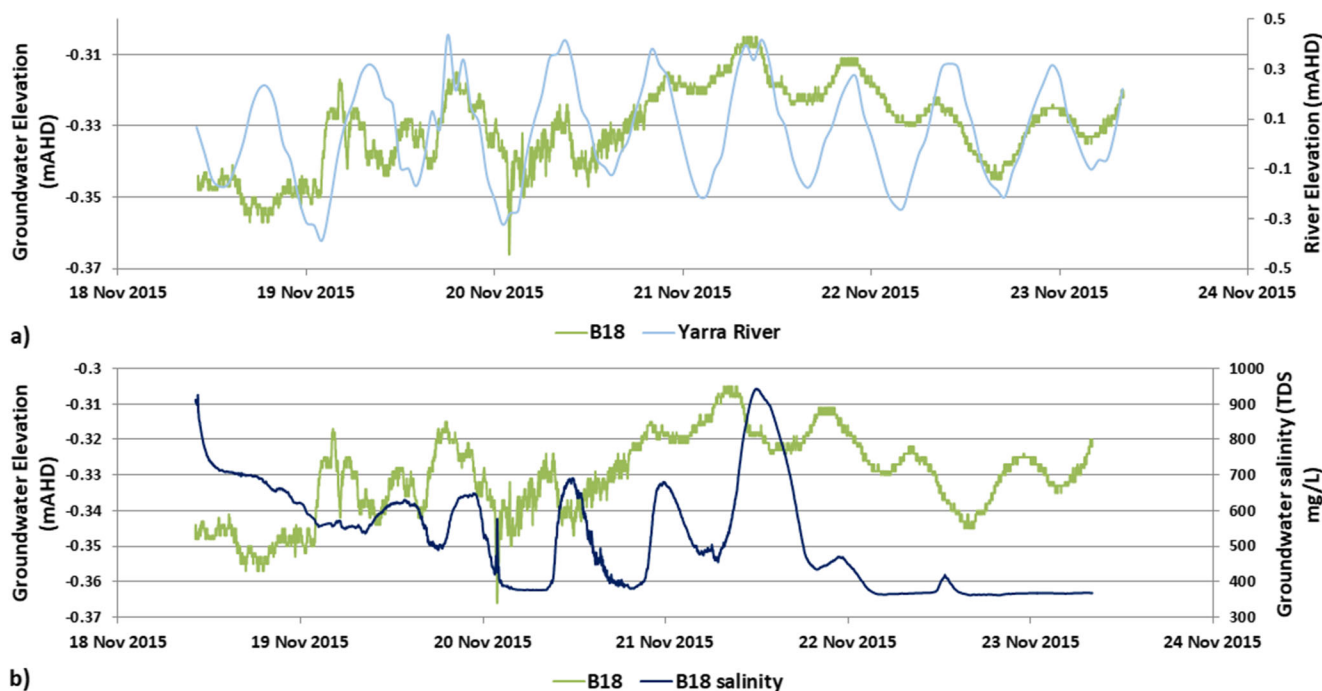

Fig. 4 **a** Hydrograph for bore B18 located 460 m from the Yarra River within the Port Melbourne Sand aquifer over a 5-day period, including Yarra River elevation (source: Melbourne Water 2018); **b** Groundwater level and salinity in bore B18 over a 5-day period

Fig. 5 Cross section C–D showing the Yarra River, bores CIS1 and B18, including screened interval positions and TDS values at high and low river levels. Bore screen intervals are marked using horizontal lines
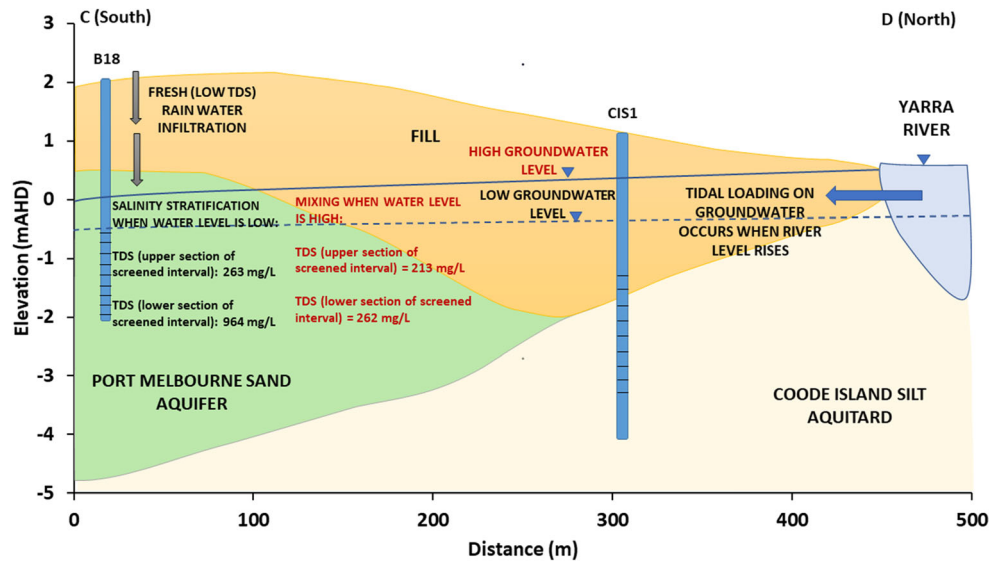
Groundwater salinity and major ion chemistry

Groundwater salinity and major ion chemistries for the Port Melbourne Sand aquifer and the Coode Island Silt aquitard are presented in Table 1 and Fig. 7. Most of the groundwater in the Port Melbourne Sand and transitional material (described in section 'Geology and hydrogeology') was Ca-HCO$_3^-$ dominant, with some Ca-SO$_4^{2-}$ and

Na-HCO$_3^-$ dominant groundwater in localised areas (e.g. B26, and B1 and B2, respectively). Molar Na/Cl, Mg/Cl and Ca/Cl ratios in the Port Melbourne Sand and transitional material were highly variable, ranging from 0.71 to 5.65, from 0.13 to 3.69, and from 0.03 to 22.66, respectively (Fig. 7). Groundwater salinity in the aquifer was fresh to brackish, ranging from 189 to 3,680 mg/L TDS (Table 1).
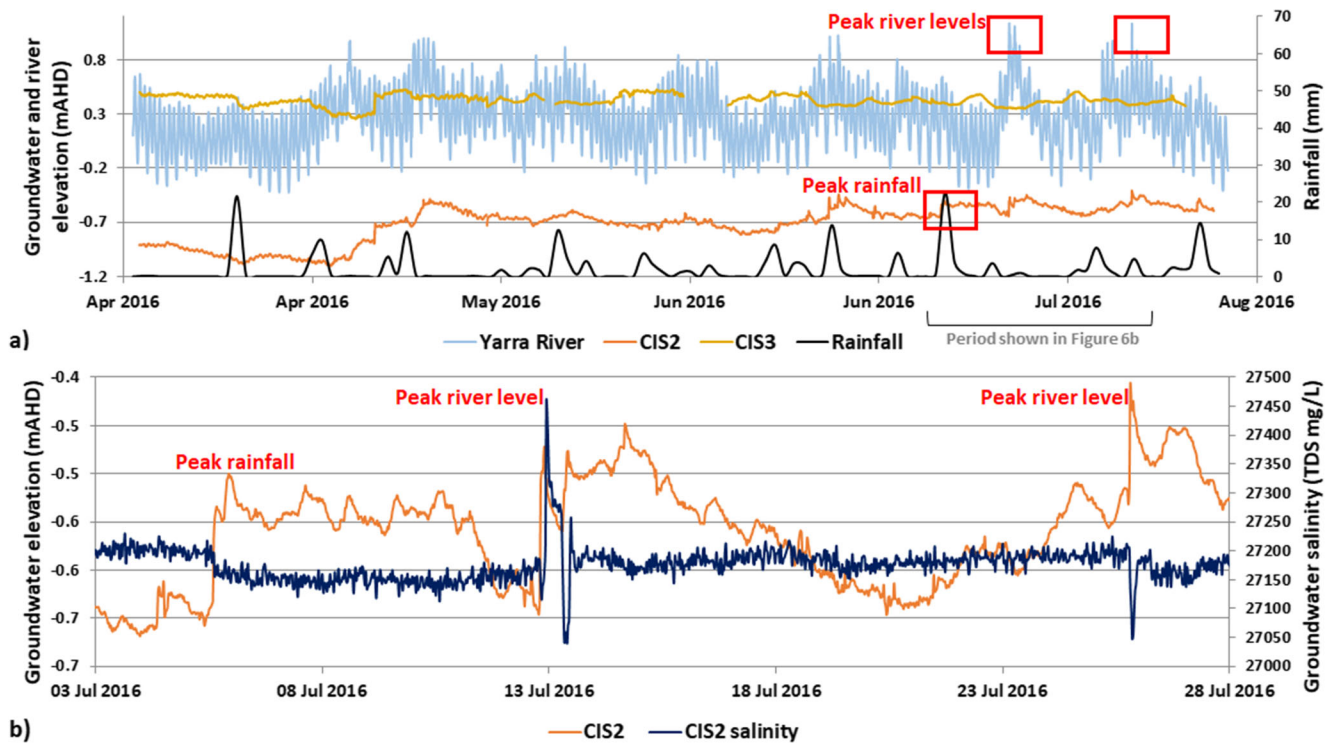
Fig. 6 **a** Hydrographs for two bores located within 280 m from the Yarra River in the Coode Island Silt aquitard over a 4-month period, including daily rainfall (source: BOM 2018) and Yarra River elevation (source: Melbourne Water 2018); **b** Groundwater level and salinity in bore CIS2 over a 25-day period (3 July to 28 July 2016) in which rainfall and river levels peaked. Peak rainfall occurred over a 2-day period between 6 and 7 July 2016 with a total of 26.4 mm

**Fig. 7** Piper diagram showing major ion compositions of groundwater
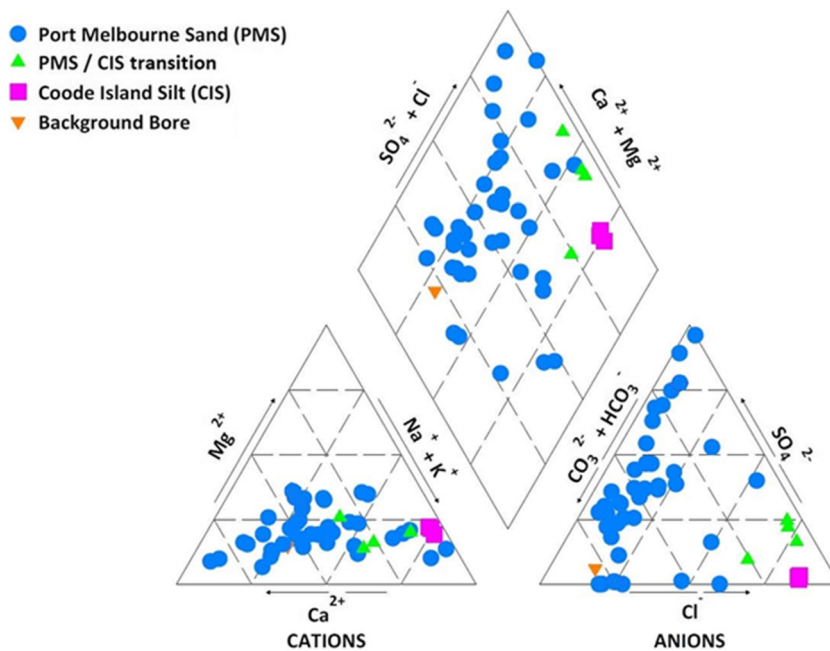
All bores screened in and partially in the Coode Island Silt contained Na-Cl-dominant groundwater (Fig. 7). Bores located within 300 m of the Yarra River (Fig. 1) and screened completely in the Coode Island Silt (CIS1–CIS3) contained saline groundwater which ranged from 19,600 to 23,900 mg/L TDS (mean = 22,000 mg/L TDS). Molar Na/Cl, Mg/Cl and Ca/Cl ratios in these bores were consistent with ocean water composition (Appelo and Postma 2005; Fig. 7). Similarly, bores screened in or partially in the Coode Island Silt and located within 600 m of the Yarra River (CIS4, CIS5, CIS6; Fig. 1) contained brackish groundwater which ranged between 2,200 and 8,390 mg/L TDS (Table 1). Molar Na/Cl, Mg/Cl and Ca/Cl ratios in these bores also reflect typical ocean water, but with some Ca-enrichment (Fig. 7). Molar ratios in these bores plot between those of the Port Melbourne Sand and those of the Coode Island Silt (Fig. 7) providing evidence of mixing between the two units. In addition, elevated concentrations of potassium (range: 1.13–2.53 mmol/L) and chloride (range: 23–136 mmol/L) relative to the Port Melbourne Sand aquifer were detected (Table 1).

One background bore (B) located in the north of the study area upgradient from any known contamination sources, contained the freshest groundwater (TDS = 143 mg/L; Table 1; Fig. 1). The groundwater in this bore was Ca-HCO_3^- dominant (Fig. 7) and molar Na/Cl, Mg/Cl and Ca/Cl ratios were 1.82, 0.53 and 2.01, respectively (Fig. 8). These results are interpreted as representing typical rainfall recharge-derived ionic ratios, with minimal influence from marine water ingress or contamination sources.

Isotopic data: $\delta^{18}O$, δ^2H, $\delta^{13}C$, tritium and radiocarbon

Stable isotopic compositions of groundwater across Fishermans Bend are shown in Table 1 and Fig. 8, along with the Melbourne winter and summer local meteoric water lines (LMWL), the global meteoric water line (GMWL), local rainfall values based on precipitation amount, and standard oceanic water (VSMOW). Stable isotopic compositions within the Port Melbourne Sand aquifer ranged from −5.7 to −2.9‰ for $\delta^{18}O$ and from −32.5 to −14.9‰ for δ^2H, generally plotting on or between the winter and summer LMWL. Most groundwater samples in the Port Melbourne Sand plotted close to the weighted mean composition of rainwater for Melbourne (−4.7‰ $\delta^{18}O$ and −25.8‰ δ^2H) or slightly higher, likely due to minor evaporation. These samples plot along a least-squares regression trend line with a slope of ~5.8, consistent with evaporative enrichment; although, the slope is also consistent with what would be expected due to marine water mixing. Significant mixing with marine water in the majority of these samples can be ruled out on the basis of the low salinity (see the following). Stable isotopic compositions within the Coode Island Silt ranged from −3.8 to −3.1‰ for $\delta^{18}O$ and from −21.7 to −18.3‰ for δ^2H, showing enrichment in comparison to the Port Melbourne Sand. The values plot along an approximate trend line between the Melbourne average weighted rainfall and the values of the Yarra River and standard oceanic water (which are similar), indicating mixing between these sources. Such mixing is also consistent with salinity data—although with an enrichment in the chloride values in the CIS groundwater, indicating a further source

Fig. 8 Ion ratios in groundwater: **a** Na/Cl; **b** Mg/Cl; **c** Ca/Cl. Standard ocean water composition taken from Appelo and Postma ([2005](#))
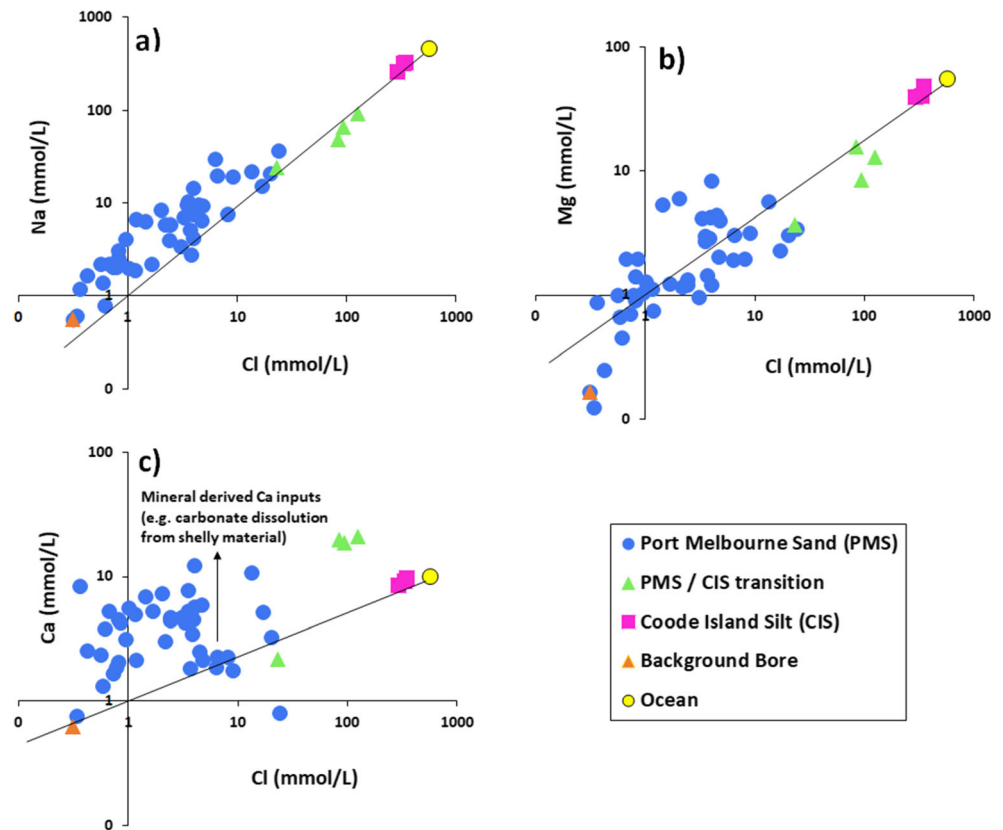
of salinity that does not enrich the stable isotope values. The compositions of groundwater from bores screened partially in the Coode Island Silt ranged from −4.1 to −3.9‰ for $\delta^{18}O$ and from −22.3 to −21.6‰ for δ^2H, plotting between those of the Port Melbourne Sand and the Coode Island Silt. These samples are likely enriched compared to those from the Port Melbourne Sand due to some combination of evaporation and mixing with oceanic water.

Tritium activities in the Port Melbourne Sand aquifer ranged from 1.75 to 2.45 TU (Table [2](#)), similar to Melbourne rainfall (2.8–3.0 TU; Tadros et al. [2014](#)) but with some minor decay and/or mixing with low-tritium containing water. In contrast, tritium activities in the Coode Island Silt aquitard ranged from 0.20 to 0.35 TU, which is significantly lower, although a minor component of recent/modern recharge is indicated. While the analytical uncertainty in the quantification of tritium at these levels is relative in comparison to the values, the results are clearly above the quantification limit for tritium, indicating (at the qualitative level) the presence of a minor component of modern water. Radiocarbon activities in the Port Melbourne Sand aquifer ranged from 31.14 to 83.94 pMC and from 35.97 to 72.79 pMC in the Coode Island Silt aquitard (Table [2](#)). Dissolved inorganic carbon (DIC) isotope ($\delta^{13}C_{DIC}$) values in the Port Melbourne Sand ranged from −19.4 to −4.2‰ with one exception of +7.9‰ at bore B2 (impacted by nearby municipal

landfills—see Fig. [1](#) and section 'Contamination inputs'). $\delta^{13}C_{DIC}$ values in the Coode Island Silt were slightly higher than those of the aquifer and ranged from −13.3 to −4.2‰ (median = −11.0‰). Dissolved methane (CH_4) in groundwater in the Port Melbourne Sand and transitional material ranged from <0.01 to 10 mg/L and from 0.03 to 1.41 mg/L in the Coode Island Silt; methanogenesis is, thus, a likely influence on the $\delta^{13}C_{DIC}$ values.

Discussion

Controls on groundwater salinity and major ion geochemistry

The major processes and sources of solutes which control groundwater salinity and major ion geochemistry at Fishermans Bend are discussed in the following and include: (1) rainfall recharge, (2) contamination inputs, (3) emplacement and flushing of relict solutes, and (4) mixing with surface waters.

Rainfall recharge

Groundwater in the Port Melbourne Sand is predominantly recharged by rainfall, indicated by hydrographs which

demonstrate positive correlations between groundwater level and rainfall (Fig. 3), relatively high ³H activities (Table 2), fresh to brackish salinity (Table 1), $\delta^{18}O$ values from −5.7 to −2.9‰, and $\delta^{2}H$ values from −32.5 to −14.9‰ (Fig. 9). No additional ³H sourced from legacy landfills is expected to be present in groundwater as waste acceptance ceased prior to the 1990s and no spatial correlations were found between ³H activities in groundwater and legacy landfill location. Stable isotopic compositions of most PMS groundwater samples plotted similar to or slightly higher than the isotopic values associated with rainfall events between 5 and 150 mm, indicating that the majority of rainfall recharges the aquifer, regardless of precipitation amount (Fig. 9). Evidence of evaporation of shallow groundwater within the Port Melbourne Sand (likely during recharge infiltration) is shown on Fig. 10 which depicts the expected Cl and ¹⁸O values for mixing and evaporation trajectories. The majority of samples in the PMS are far to the left of the expected mixing trajectory between the Yarra River and Melbourne rainfall and have significantly higher $\delta^{18}O$ values per unit increase in Cl than would be expected if mixing with (saline, marine-influenced) Yarra River water was occurring. This is supported by Cl mixing proportions for the majority of samples in the PMS of between 0.05 and 6%, versus elevated $\delta^{18}O$ mixing proportions for the same samples of between 6 and 56%, indicative of evaporation-induced fractionation of $\delta^{18}O$. The impact of evaporation on groundwater within the PMS is in clear contrast to groundwater from the CIS and transitional (PMS/CIS) material which indicate mixing to various proportions with Yarra River water (Fig. 10; see also section 'Mixing with surface waters').

Contamination inputs

Localised areas of brackish salinity and Ca-SO$_4^{2−}$ dominant groundwater in the Port Melbourne Sand were generally associated with impacts from former industrial

activities; for example, at bore B26 which is located immediately down-gradient from a former metal foundry and had a pH of 2.96 and a TDS value of 1,460 mg/L in May 2016 (Table 1), and has previously contained elevated concentrations of heavy metals (Hepburn et al. 2018). In addition, localised areas of brackish salinity and Na-HCO$_3^−$ dominant groundwater were generally associated with legacy landfill leachate impacts, for example at bores B1 and B2 which are located near municipal legacy landfills and had TDS values of 3,680 and 2,240 mg/L, respectively, including elevated concentrations of ammonia-N, potassium and dissolved methane relative to the median values reported for the Port Melbourne Sand (Hepburn et al. 2019b).

Emplacement and flushing of relict solutes

The Na-Cl dominant groundwater in the Coode Island Silt, in combination with saline water and molar ratios within the typical range for ocean water, indicate that solutes are predominantly of marine origin, consistent with groundwater recharged by direct emplacement of marine water, as found in a similar coastal setting by Lee et al. (2016). Given the low hydraulic conductivity of the Coode Island Silt, the residence times of these emplaced salts are likely to be in the order of thousands of years, driven by the gradual flushing and replacing of saline pore water (sourced from the estuary) within this unit.

In more recent times, the geochemistry of the Coode Island Silt may have been influenced by significant changes to the course of the adjacent Yarra River. In 1879, a natural rock bar which separated fresh river water from saline ocean water was blasted in order to widen the river to alleviate floods (Melbourne Water 2017). The effect of this was to allow fresh/saline waters to mix, and a saline wedge subsequently

Fig. 9 Stable isotope compositions of groundwater collected in May 2016 and May 2017. Local meteoric water line (LMWL) and rainfall data collected between 1960 and 2014 from the IAEA-WMO Global Network for Isotopes in Precipitation and calculated following Hollins et al. (2018). GMWL is global meteoric water level
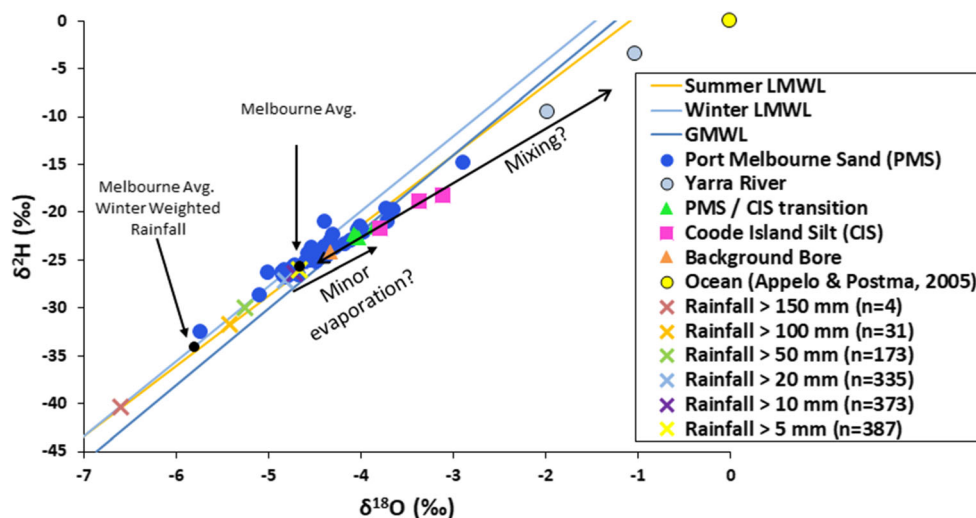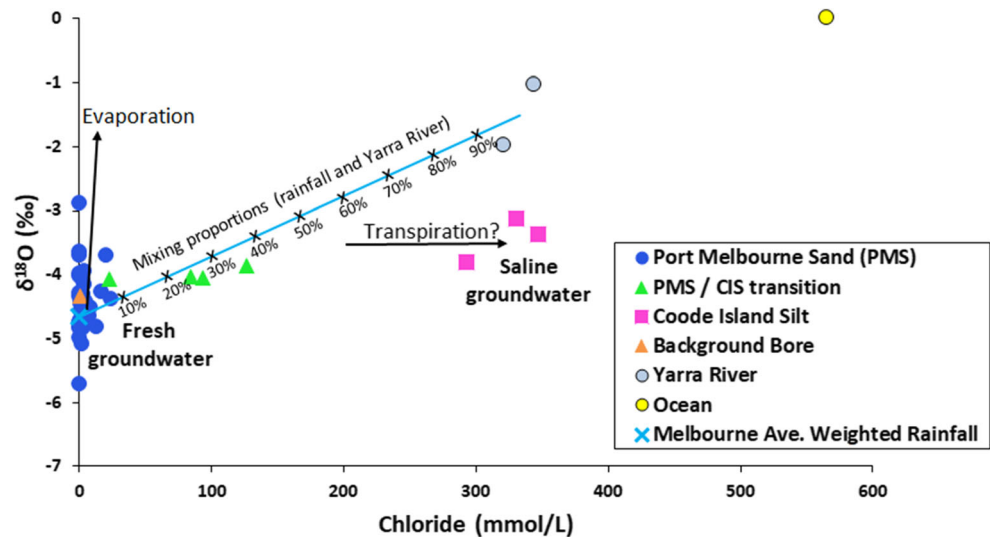
Fig. 10 Stable isotopic compositions and salinities of groundwater, indicating water and salinity sources, and inferred mixing proportions between Melbourne average weighted rainfall and the Yarra River. Evaporation trend line is indicative only

formed at the base of the river (EPA Victoria 2013). A short time later in 1883, the City of Melbourne began construction of its sewer system, with various sewers constructed throughout the study area (AECOM 2015). The subsequent abandonment of these sewers over time has led to integrity issues resulting in groundwater sinks in-land, which have subsequently increased hydraulic gradients between the Yarra River and the groundwater. Saline groundwater was generally found within the aquitard in bores closest to the river (CIS1, CIS2 and CIS3), with molar ratios consistent with typical ocean water (section 'Controls on groundwater carbon geochemistry'). In contrast, bores screened in or partially in the Coode Island Silt and located within 600 m of the river contain brackish salinity and molar ratios similar to typical sea water but with some Ca-enrichment, likely reflecting inputs from dissolution of carbonate-rich shell material most commonly present at the base of the Port Melbourne Sand and in the Coode Island Silt (see section 'Controls on groundwater carbon geochemistry', and the following).

Mixing with surface waters

A limited component of modern recharge water is present in the Coode Island Silt, as indicated by the presence of tritium above background levels. Given the small outcrop area of the Coode Island Silt (Fig. 1) and the low hydraulic conductivity (section 'Groundwater flow direction, levels and hydraulic conductivities'), this modern water is unlikely to be sourced from direct recharge by modern rainfall. This is consistent with only minor freshening of the aquitard observed during peak rainfall (Fig. 6b), attributable to an increase in vertical hydraulic gradient between the aquifer and the aquitard, allowing inter-aquifer leakage from the Port Melbourne Sand (via transitional material) into the Coode Island Silt. Instead, Fig. 10 provides evidence for mixing between the

Coode Island Silt and the Yarra River, indicating that the most likely source of modern recharge to the aquitard is ingress from the river. This is supported by $\delta^{18}O$ mixing proportions of between 27 and 49% river water in the Coode Island Silt groundwater (Fig. 10; method described in section 'Groundwater salinity and major ion chemistry') consistent with the salinity fluctuations following peak river levels (see section 'Controls on groundwater carbon geochemistry'), when hydraulic head differentials between the river and the aquitard were greatest (Fig. 6b). Further salinization of groundwater within the Coode Island Silt is also evident in Fig. 10 and is shown by deviation to the right of the mixing trajectory. This is interpreted as reflecting mixing with a hypersaline end-member, possibly linked to solute concentration by transpiration, via coastal vegetation—likely associated with former swampy areas (see Fig. 1). A similar effect was reported by Lee et al. (2016), who showed that chloride and stable isotope values of saline groundwater emplaced during the mid-Holocene could only be explained by mixing between a fresh meteoric end-member and a hyper-saline end-member with limited $\delta^{18}O$ and $\delta^{2}H$ enrichment. The major processes and sources of solutes which control groundwater salinity and major ion geochemistry at Fishermans Bend are summarised in Fig. 11.

Controls on groundwater carbon geochemistry

Accounting for the physico-chemical characteristics of the groundwater at Fishermans Bend (e.g. pH and alkalinity), the typical range of $\delta^{13}C_{DIC}$ in groundwater where the majority of DIC is sourced from C3 vegetation should range between −17.4 and −11.4‰ (mean −14.4‰; Clark and Fritz 1997). The $\delta^{13}C_{DIC}$ values in the Port Melbourne Sand typically ranged from −19.4 to −4.2‰ and from −13.3 to −4.2‰ in the Coode Island Silt (Table 2). Analysis of $\delta^{13}C_{DIC}$, ^{14}C,
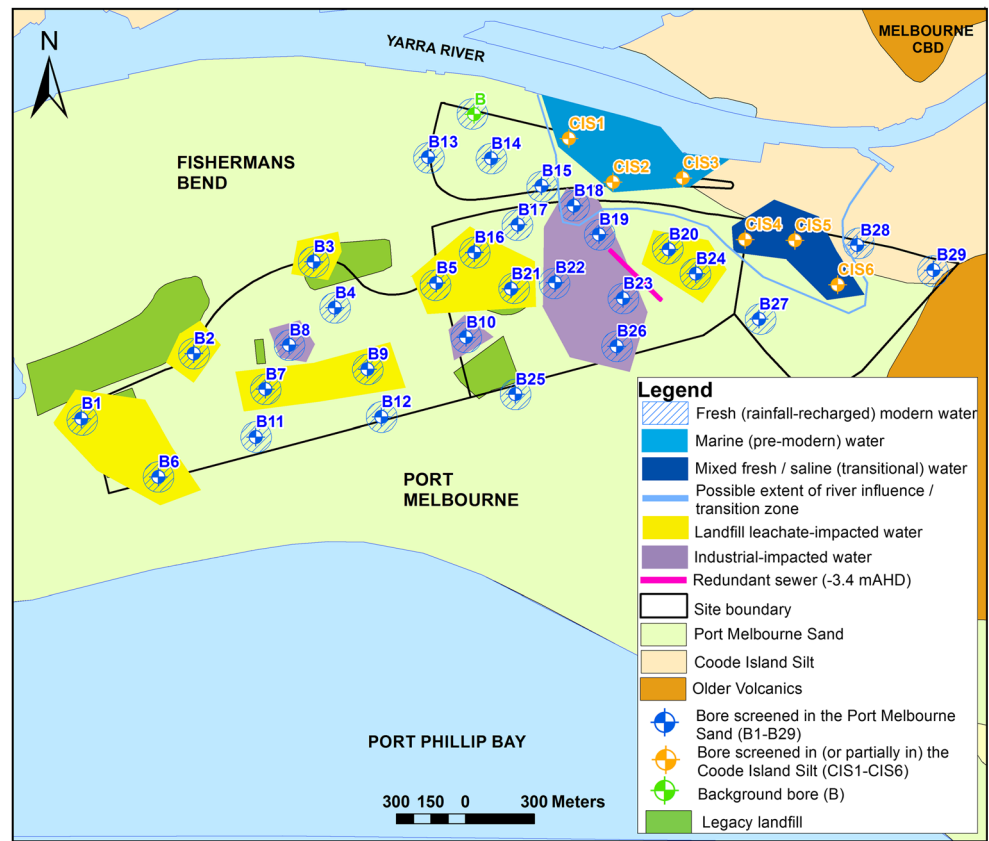
^{3}H and the enrichment/depletion of major ions in groundwater across Fishermans Bend has helped constrain residence times and identified the processes accounting for enrichment of $\delta^{13}C_{DIC}$, including: (1) decay of organic waste and methanogenesis in landfill leachate-impacted bores, and (2) carbonate dissolution from shell material (Fig. 1). These processes are analysed with the aid of Fig. 12 and are discussed further on.

Landfill leachate inputs

Bores B6 and B7 have previously been shown to be impacted by landfill leachate generated by legacy municipal landfills present in the west of the study area (see Fig. 1; Hepburn et al. 2019b). This was supported by elevated HCO_3^- (18.2 mmol/L in B6 and 15.4 mmol/L in B7) and K^+ (1.89 mmol/L in B6 and 0.79 mmol/L in B7; relative to the background bore, Table 1), which are typically enriched in landfill leachates (Kjeldsen et al. 2002). Enriched $\delta^{13}C_{DIC}$ values in these bores (e.g. –9.3‰ in B6 and –6.0‰ in B7) suggest that degradation of organic waste has produced ^{13}C-enriched CO_2 which has mixed with the comparatively depleted natural soil CO_2 (typical mean $\delta^{13}C_{DIC}$ in soil CO_2 derived from C3 plants equals −23‰; Clark and Fritz 1997), thereby enriching the $\delta^{13}C_{DIC}$. Cartwright et al. (2010) found that elevated HCO_3^- generated as a by-product of methanogenesis

by bacterial reduction, will also enrich $\delta^{13}C_{DIC}$ values. Evidence for this process occurring in bores B1 and B2 (impacted by the same municipal landfills in the west of the

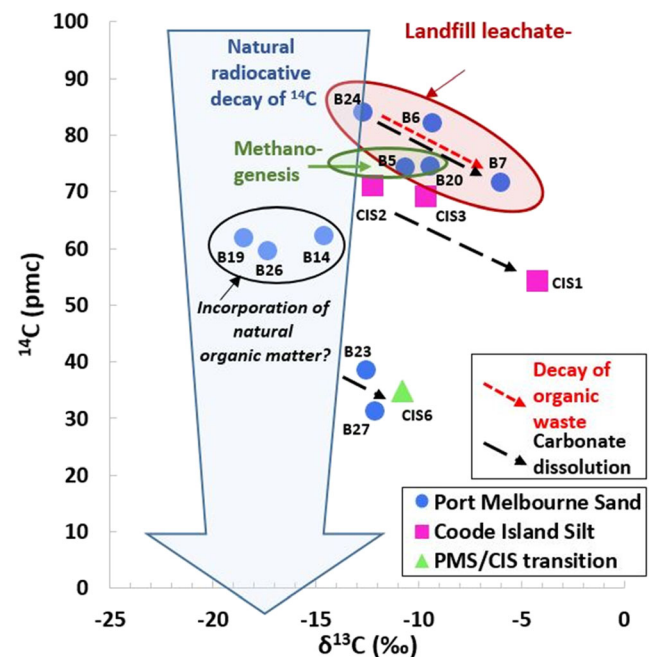Fig. 12 $\delta^{13}C_{DIC}$ versus ^{14}C for groundwater samples indicating influences from carbonate dissolution, decay of old organic waste and methanogenesis

study area; see Fig. 1 and Hepburn et al. 2019b) includes enriched $\delta^{13}C_{DIC}$ values of −4.2 and +7.9‰ (Table 2), and enriched bicarbonate values of 26.9 and 23.9 mmol/L (Table 1), respectively. Significantly elevated concentrations of dissolved methane in bores B1 and B2 (3.9 and 10 mg/L, respectively), and low sulfate concentrations (0.31 and 0.01 mmol/L, respectively), indicate biogenic methanogenesis is occurring in these groundwaters and is likely responsible for the enriched HCO_3^- (and subsequent enriched $\delta^{13}C_{DIC}$; Clark and Fritz 1997).

Further evidence for $\delta^{13}C_{DIC}$ enrichment was also found, to a lesser extent, in groundwater impacted by leachate from landfills inferred to contain industrial, construction and/or demolition waste (bores B5, B20 and B24; see Fig. 1 and Hepburn et al. 2019b). These bores have slightly enriched $\delta^{13}C_{DIC}$ values of −10.6, −9.4 and –12.7‰, respectively (Table 2). Dissolved methane concentrations in bores B5 and B20 were significantly elevated (10 and 7.6 mg/L, respectively) as were bicarbonate concentrations (18.3 and 13.5 mmol/L), while sulfate concentrations were low (0.01 mmol/L in both bores). These results provide evidence that biogenic methanogenesis is occurring in the groundwater at these locations, which suggests that that some domestic (organic) waste was deposited in the landfills, and that the enriched $\delta^{13}C_{DIC}$ are partially derived from enriched HCO_3^- generated during methanogenesis (Clark and Fritz 1997). Groundwaters in bores B5 and B20 were $Na-HCO_3^-$ and Na-Cl dominant, respectively, indicating that release of some sodium from the waste is occurring, as might be expected in later stage leachate plumes (Mulvey 1999). Overall, these results suggest that the breakdown of organic waste within legacy landfills still controls the surrounding groundwater $\delta^{13}C_{DIC}$ values after at least ~30 years since landfill closure, and several drought–wet cycles. Similar findings were obtained by Cendón et al. (2015) who noted that groundwater affected by interaction with waste will vary depending on the type of waste, the time since disposal (maturity) as well as the various bacterial reduction processes involved. More broadly, the data show how a combination of carbon stable isotopes and concentrations of key analytes that are sensitive to landfill impact—e.g. bicarbonate, sodium and dissolved methane—can be used to identify solutes in groundwater derived from legacy landfill sites, as opposed to other sources.

[14]C values in the five bores impacted by landfill leachate (bores B5, B6, B7, B20 and B24) ranged from 71.65 to 83.94 pMC (Table 2; Fig. 12); however, the presence of ^{3}H in these bores (range: 1.75–2.13 TU; Table 2) indicates active recharge by modern Melbourne rainfall (Tadros et al. 2014) and suggests that ^{14}C values have been lowered by incorporation of carbon from the decay of organic wastes and methanogenesis, as already discussed. In addition, carbonate dissolution from abundant shell material noted in the lower beds of the Port Melbourne Sand in bore B7 has likely contributed dead

carbon (Clark and Fritz 1997) to the groundwater at this location, in addition to enriching the $\delta^{13}C_{DIC}$ values (Fig. 12; see further discussion of carbonate dissolution in the following). Due to these complications (further discussed in the following) a decision was made not to attempt to calculate groundwater residence times using the ^{14}C data, for example using correction schemes based on $\delta^{13}C_{DIC}$ (Clark and Fritz 1997).

Carbonate dissolution

The Na/Cl dominant groundwater within the Coode Island Silt (bores CIS1, CIS2, CIS3 and CIS6) in combination with molar ratios representative of typical ocean water, suggest that the enriched $\delta^{13}C_{DIC}$ values evident in these groundwaters (range: −13.3 to −4.2‰, mean = −10.3‰; Table 2; Fig. 12) are derived from marine carbonates such as shell material commonly present within the aquitard (see Fig. S3 of the ESM). $\delta^{13}C_{DIC}$ values within shell material collected from the upper and lower Port Melbourne Sand, and the Coode Island Silt, have previously been reported to be between −1.1 and + 1.2‰ (Holdgate and Norvick 2017). These results suggest that the dissolution of shell material would be expected to contribute DIC with a $\delta^{13}C_{DIC}$ value closer to 0‰. Therefore, the intermediate $\delta^{13}C_{DIC}$ values evident in these bores suggest some combination of soil-derived CO_2 (typical mean $\delta^{13}C_{DIC}$ in soil CO_2 derived from C3 plants equals −23‰; Clark and Fritz 1997) and some dead carbon derived from shell dissolution.

[14]C values in bores screened completely within the Coode Island Silt (CIS1, CIS2 and CIS3) were 56.54, 72.29 and 71.30 pMC, respectively. The presence of minor amounts of ^{3}H in these bores (0.20, 0.25 and 0.35 TU, respectively) again indicates that modern recharge is present in the aquitard, but that it constitutes a limited component of the total water in the system. The ^{14}C values may therefore be a reasonable representation of groundwater residence times in the aquitard (i.e. water emplacement having occurred in the late Holocene); however, the dissolution of shell material and incorporation of old organic matter (e.g. from former swampy areas, see Fig. 1) have likely contributed to lowering the ^{14}C values somewhat. In addition, contamination sources (e.g. hydrocarbon odours and gasworks waste) noted in the fill at CIS6 have likely resulted in further lowering the ^{14}C value to 35.97 pMC (Table 2) by contributing dead carbon from decaying organic contaminants. The tritium concentration of 2.27 TU in this bore indicates active recharge by modern Melbourne rainfall (Tadros et al. 2014).

Evidence for carbonate dissolution was also found in two bores screened towards the base of the Port Melbourne Sand (B23 and B27), where significant shell beds were recorded in the borehole logs and enriched $\delta^{13}C_{DIC}$ values of −12.5 and –12.1‰ were observed, respectively. At bore B23, metal concentrations in natural sediment (measured using X-ray fluorescence following the method outlined in Hepburn et al.

2018), yielded Ca concentrations between 70 and 620 mg/kg in the upper Port Melbourne Sand where shell beds were absent, and concentrations between 1,100 and 6,600 mg/kg in the lower, shell-rich beds. At bore B27, Ca concentrations in the upper natural sediment ranged from 330 to 900 mg/kg, compared to concentrations between 6,700 and 7,600 mg/kg in the lower, shell-rich beds. The Ca/Cl ratios in both bores were enriched (Ca/Cl = 0.28 in B23 and 5.43 in B27) relative to typical ocean water (Ca/Cl = 0.02; Appelo and Postma 2005), potentially due to excess Ca from carbonate dissolution. The particularly low ^{14}C values in bores B23 and B27 (38.59 and 31.14 pMC, respectively; Table 2) were likely impacted by dead carbon from these shells; these results are relatively consistent with values obtained from shell material within the lower Port Melbourne Sand (39.6 and 40.4 pMC) by Holdgate and Norvick (2017).

Within the Port Melbourne Sand aquifer, enriched $\delta^{13}C_{DIC}$ values in bores where shell beds are present and carbonate dissolution is likely occurring (bores B16, B21, B22, B23, B27 and B29; see Table 2) can be distinguished from enrichment due to methanogenesis/organic waste decay by assessment of the Ca/Cl and K/Cl ratios. Where carbonate dissolution enriches the $\delta^{13}C_{DIC}$ values, the mean Ca/Cl ratio is 6.21 (range: 0.28–22.66), indicating excess Ca in the groundwater, and the mean K/Cl ratio is 0.31 (range: 0.08–0.56), indicating minimal K excess. In contrast, where methanogenesis/organic waste decay has enriched the $\delta^{13}C_{DIC}$ values, the mean Ca/Cl ratio is significantly lower (mean = 0.34, range: 0.03–0.87), indicating a lack of Ca excess as expected where shell beds are absent, and the K/Cl ratio is slightly lower (0.14) indicating elevated concentrations of both K and Cl (demonstrated in Table 1), as expected in late stage leachate-impacted groundwaters (Mulvey 1999). Bores B7 and B9, which are impacted by both landfill leachate and the presence of shell beds, have intermediate Ca/Cl ratios of 1.38 and 1.89, respectively, and intermediate K/Cl ratios of 0.14 and 0.25, respectively.

$\delta^{13}C_{DIC}$ values at bores B14, B19 and B26 (−14.6, −18.5 and −17.3‰, respectively; Table 2) were typically within the expected range for Fishermans Bend groundwater not impacted by carbonate dissolution and methanogenesis (i.e. −17.4 to −11.4‰, see the preceding), indicating little $\delta^{13}C_{DIC}$ enrichment, consistent with a lack of landfill leachate impact and the general absence of visible shell material within these bores (Fig. 12). ^{14}C values, however, ranged from 59.45 to 62.11 pMC, whilst tritium concentrations ranged from 1.88 to 2.45 TU, indicating recharge by modern rainfall (Tadros et al. 2014), along with significant input of dead carbon. One explanation for the low ^{14}C values observed in bores B14 and B19 may be the presence of dead organic matter generated within the former swampy areas, within which these bores are located (see Fig. 1). An explanation for the low ^{14}C values at B26 is unclear; however, this bore is significantly impacted by industrial activities (see section 'Contamination inputs'),

which may potentially have resulted in some petroleum hydrocarbon (i.e. dead carbon) impacts to groundwater.

Conclusions

The coastal area of Fishermans Bend is currently undergoing progressive redevelopment from industrial to medium- and high-density residential land. Understanding the hydrogeological system at Fishermans Bend is important for effectively characterising the impacts from legacy contamination and monitoring the effects of urbanisation on groundwater flow systems and quality. A range of isotopic (δ^{18}O, δ^2H, δ^{13}C, ^{3}H and ^{14}C) and geochemical indicators (major ions) were analysed in the shallow groundwater at Fishermans Bend, in order to determine sources of water salinity in the Port Melbourne Sand aquifer and the Coode Island Silt aquitard. Groundwater in the Port Melbourne Sand was Ca-HCO$_3^-$ dominant, with salinity ranging from fresh to brackish. Localised areas of Ca-SO$_4^{2-}$ and Na-HCO$_3^-$ dominant groundwater were typically impacted by industrial activities and legacy landfills, respectively. Hydrographs, stable isotopes and tritium activities within the aquifer indicate meteoric water recharged by modern rainfall, with short residence times. In addition, hydrographs from one bore located proximal to the Yarra River showed tidal influence from the river, which eventually connects to the Southern Ocean. Carbonate dissolution from shell material, and decay of organic waste and methanogenesis in landfill leachate-impacted bores were shown to enrich δ^{13}C values.

In contrast, groundwater in the adjacent/lower aquitard was Na-Cl dominant and saline, with molar ratios reflective of typical ocean water, indicating relict salts emplaced as porewater at the time of sediment deposition. ^{14}C dating of shell material indicates this unit was deposited in a marine environment during the middle-Holocene (Holdgate and Norvick 2017). The solute composition and radiocarbon activities in groundwater (pMC values between 56.54 and 72.79) are consistent with this interpretation; however, the presence of tritium above background levels suggest some (small) component of modern recharge as well. Hydrographs, stable isotopes and salinity fluctuations within the aquitard at times of peak river level suggest the source of this modern recharge is likely to be ingress from the adjacent Yarra River. Further targeted high-frequency monitoring of river and groundwater levels and hydrochemical composition may allow a more precise understanding of these ground/surface-water dynamics to be attained.

The findings of this study have important practical implications for the major land redevelopment planned for Fishermans Bend. As the land is redeveloped, assessments will be made with respect to the extent and degree of groundwater contamination from past land-uses. The data and

findings regarding the dominant solute origins and hydrochemical processes impacting groundwater quality will assist in identifying natural influences as distinct from site-based contamination. The findings regarding recharge and residence times also have implications for the future remediation of contaminated groundwater—e.g., knowing that rapid, active recharge occurs in the upper aquifer can assist in the design of treatment systems which (for example) make use of the relatively rapid flushing of the aquifer.

Additionally, this study has provided a template regarding how environmental isotopes can be used to constrain solute origins in coastal aquifers impacted by contamination and ground/surface-water interaction. The stable isotopes of water, in combination with tritium, were effective in identifying the degree of mixing between groundwater in the two primary units, as well as input from river water. Stable isotopes of carbon were particularly useful (in conjunction with major ions) at identifying groundwater impacted by landfill leachate from legacy sites in the precinct. Radiocarbon was effective in constraining the timescales of marine water emplacement (e.g. during deposition of the marine sediments in the mid-Holocene) and along with tritium, showed that recharge occurred on very different timescales within the two aquifers; associated with very different hydrochemical signatures.

References

AECOM (2015) Desktop study and preliminary regional conceptual site model, Fishermans Bend urban renewal area. Report for EPA Victoria. http://www.epa.vic.gov.au/our-work/programs/~/media/Files/Ourwork/Programsandinitiatives/FishermansBend/FINAL-FBURA-Desktop-Study_Aug-2015.pdf. Accessed 12 January 2018

AECOM (2016) Baseline groundwater quality assessment, Fishermans Bend Urban Renewal Area, Report for EPA Victoria. http://www.epa.vic.gov.au/our-work/programs/~/media/Files/Ourwork/Programsandinitiatives/FishermansBend/FINAL-FBURA-Baseline-Report_March-2016.pdf. Accessed 12 January 2018

APHA (American Public Health Association) (2017) Standards for examination of water and waste water. America Water Works Association, 23rd edn. Water Environment Federation, Washington, DC

Appelo CAJ, Postma D (2005) Geochemistry, groundwater and pollution, 2nd edn. Balkema, Dordrecht, The Netherlands, 58 pp

Assayag N, Rivé K, Ader M, Jézéquel D, Agrinier P (2006) Improved method for isotopic and quantitative analysis of dissolved inorganic carbon in natural water samples. Rapid Commun. Mass Spectrom. 20:2243–2251

Beckett R, Easton AK, Hart BT, McKelvie ID (1982) Water movement and salinity in the Yarra and Maribyrnong estuaries. Aust J Marine Freshwater Res 33:401–415

Bruce LC, Cook PLM, Hipsey MR (2011) Using a 3D hydrodynamic-biogeochemical model to compare estuarine nitrogen assimilation efficiency under anoxic and oxic conditions. 19th Int. Congress on Modelling and Simulation, Perth, Australia, pp 3691–3697

Bruce LC, Cook PLM, Teakle I, Hipsey MR (2014) Hydrodynamic controls on oxygen dynamics in a riverine salt wedge estuary, the Yarra River estuary. Australia Hydrol Earth Syst Sci 18:1397–1411

BOM (Bureau of Meteorology) (2018) http://www.bom.gov.au. Accessed 9 August 2018

Cartwright I, Weaver TR, Stone D, Reid M (2007) Constraining modern and historical recharge from bore hydrographs, ^{3}H, ^{14}C, and chloride concentrations: applications to dual-porosity aquifers in dryland salinity areas, Murray Basin, Australia. J Hydrol 332:69–92

Cartwright I, Weaver TR, Cendón DI, Swane I (2010) Environmental isotopes as indicators of inter-aquifer mixing, Wimmera region, Murray Basin, Southeast Australia. Chem Geol 277:214–226

Cendón DI, Hughes CE, Harrison JJ, Hankin SI, Johansen MP, Payne TE, Wong H, Rowling B, Vine M, Wilsher K, Guinea A, Thiruvoth S (2015) Identification of sources and processes in a low-level radioactive waste site adjacent to landfills: groundwater hydrogeochemistry and isotopes. Aust J Earth Sci 62:123–141

Christensen TH, Kjeldsen P, Bjerg PL, Jensen DL, Christensen JB, Baun A, Albrechtsen H-J, Heron G (2001) Biogeochemistry of landfill leachate plumes. Appl Geochem 16:659–718

Clark ID, Fritz P (1997) Environmental isotopes in hydrogeology. Lewis, New York, pp 111–134

Cossu R (2013) Groundwater contamination from landfill leachate: when appearances are deceiving! Waste Manag 33:1793–1794

Currell MJ, Dahlhaus P, Ii H (2015) Stable isotopes as indicators of water and salinity sources in a southeast Australian coastal wetland: identifying relict marine water, and implications for future change. Hydrogeol J 23:235–248

DELWP (Department of Environment, Land, Water and Planning) (2017) Fishermans Bend, Australia's largest urban renewal project. www.fishermansbend.vic.gov.au. Accessed 9 August 2018

EPA (Environment Protection Authority) Victoria (2013) The origin, fate and dispersion of toxicants in the lower sections of the Yarra River. Publ. no. 1529, May 2013. EPA Victoria, Melbourne, Australia

Fink D, Hotchkis M, Hua Q, Jacobsen G, Smith AM, Zoppi U, Child D, Mifsud C, van der Gaast H, Williams A, Williams M (2004) The ANTARES AMS facility at ANSTO. Nucl. Instrum. Methods Phys. Res. Sect. B Beam Interact. Mater. Atoms 223:109–115

Golder Associates (2012) Preliminary land contamination study, Fishermans Bend precinct Report for Places Victoria June 2012. http://www.fishermansbend.vic.gov.au/__data/assets/pdf_file/0035/29798/15_Volume_3_Preliminary_Land_Contamination_Study.pdf. Accessed 20 September 2018

Hancock S (1992) Groundwater and corrosivity. In: Peck WA, Neilson JL, Olds RJ, Seddon KD (eds) Engineering geology of Melbourne. Balkema, Rotterdam, pp 223–243

Han Z, Ma H, Shi G, He L, Wei L, Shi Q (2016) A review of groundwater contamination near municipal solid waste landfill sites in China. Sci Tot Environ 569–570:1255–1264

Han D, Currell MJ, Cao G, Hall B (2017) Alterations to groundwater recharge due to anthropogenic landscape change. J Hydrol 554:545–557

Hepburn E, Northway A, Bekele D, Liu G, Currell M (2018) A method for separation of heavy metal sources in urban groundwater using multiple lines of evidence. Environ Pollut 241:787–799

Hepburn E, Madden C, Szabo D, Coggan TL, Clarke B, Currell M (2019a) Contamination of groundwater with PFAS from legacy

landfills in an urban re-development precinct. Environ Pollut 248: 101–113. https://doi.org/10.1016/j.envpol.2019.02.018

Hepburn E, Northway A, Bekele D, Liu G, Currell M (2019b) Incorporating perfluoroalkyl acids (PFAA) into a geochemical index for improved delineation of legacy landfill impacts on groundwater. Sci Tot Environ 666:1198–1208. https://doi.org/10.1016/j.scitotenv.2019.02.203

Holdgate G, Norvick M (2017) Geological evolution of the Holocene Yarra Delta and its relationship with Port Phillip Bay. Aust J Earth Sci 64(3):301–318

Hollins SE, Hughes CE, Crawford J, Cendón DI, Meredith KM (2018) Rainfall isotope variations over the Australian continent: implications for hydrology and isoscape applications. Sci Tot Environ 645: 630–645

Hughes CE, Cendón DI, Harrison JJ, Hankin SI, Johansen MP, Payne TE, Vine M, Collins RN, Hoffmann EL, Loosz T (2011) Movement of a tritium plume in shallow groundwater at a legacy low-level radioactive waste disposal site in eastern Australia. J Environ Radioact 102: 943–952

Hvorslev MJ (1951) Time lag and soil permeability in ground water observations. US Army waterways Experiment Station Bull 36, Vicksburg, MI

ISO (International Organization for Standardization) (2009) Water quality: sampling, part 11: guidance on sampling of groundwaters. International Standard ISO 5667-11. International Organization for Standardization, Geneva, Switzerland

Iverach CP, Cendón DI, Meredith KT, Wilcken KM, Hankin SI, Andersen MS, Kelly BFJ (2017) A multi-tracer approach to constraining artesian groundwater discharge into an alluvial aquifer. Hydrol Earth Syst Sci 21:5953–5969

Kjeldsen P, Barlaz MA, Rooker AP, Baun A, Ledin A, Christensen TH (2002) Present and long-term composition of MSW landfill leachate: a review. Crit Rev Env Sci Tec 32(4):297–336

Kotval Z (2016) Brownfield redevelopment: why public investments can pay off. Econ Dev Q 30(3):275–282

Lee S, Currell M, Cendón DI (2016) Marine water from mid-Holocene sea level highstand trapped in a coastal aquifer: evidence from groundwater isotopes, and environmental significance. Sci Tot Environ 544:995–1007

Leonard JG (2006) Hydrogeology of the Melbourne area. Aust Geomech J 41(3):63–74

Melbourne Water (2017) History of the Yarra River. https://www.melbournewater.com.au/community-and-education/about-our-water/history-and-heritage/history-our-rivers-and-creeks/history. Accessed 23 September 2018

Melbourne Water (2018) https://www.melbournewater.com.au/water/rainfall-and-river-levels#/. Accessed 12 September 2018

Mook W, van der Plicht J (1999) Reporting ^{14}C activities and concentrations. Radiocarbon 41(3):227–39

Mulvey P (1999) Environmental monitoring of landfills. http://www.eesigroup.com/insights/environmental-monitoring-of-landfills-by-philip-mulvey-and-wendi-trotter/. Accessed 16 August 2018

Neilson JL (1992) Geology of the Yarra Delta. In: Peck WA, Neilson JL, Olds RJ, Seddon KD (eds) Engineering geology of Melbourne. Balkema, Rotterdam, pp 223–243

Price RM, Skrzypek G, Grierson PF, Swart PK, Fourqurean JW (2012) The use of stable isotopes of oxygen and hydrogen to identify water sources in two hypersaline estuaries with different hydrologic regimes. Mar Freshw Res 63:952–966

Schirmer M, Leschik S, Musolff A (2013) Current research in urban hydrogeology: a review. Adv Water Res 51:280–291

Siegel DI, Glaser PH, So J, Janecky DR (2006) The dynamic balance between organic acids and circumneutral groundwater in a large boreal peat basin. J Hydrol 320:421–431

Smith JD, Milne PJ (1979) Determination of iron in suspended matter and sediments of the Yarra River estuary, and the distribution of copper, lead, zinc and manganese in the sediments. Aust J Marine Freshwater Res 30:731–739

Stuiver M, Polach A (1977) Reporting of ^{14}C data. Radiocarbon. 19:355–363

Tadros CV, Hughes CE, Crawford J, Hollins SE, Chisari R (2014) Tritium in Australian precipitation: a 50 year record. J Hydrol 513:262–273

UN (United Nations) (2018) 2018 Revision of World Urbanization Prospects. Dept. of Economic and Social Affairs, Population Division. https://www.un.org/development/desa/publications/2018-revision-of-world-urbanization-prospects.html. Accessed 16 August 2018

USEPA (United States Environment Protection Agency) (2018) Overview of the Brownfields program. https://www.epa.gov/brownfields/overview-brownfields-program. Accessed 11 July 2018

Vázquez-Suñé E, Carrera J, Tubau I, Sánchez-Vila X, Soler A (2010) An approach to identify urban groundwater recharge. Hydrol Earth Syst Sci 14:2085–2097

Yeh H-F, Lin H-I, Lee C-H, Hsu K-C, Wu C-S (2014) Identifying seasonal groundwater recharge using environmental stable isotopes. Water 6:2849–2861